

Exchange coupling mechanisms at ferromagnetic/CoO interfaces

F. T. Parker

Center for Magnetic Recording Research, University of California—San Diego, La Jolla, California 92093-0401

Kentaro Takano* and A. E. Berkowitz

Center for Magnetic Recording Research and Department of Physics, University of California—San Diego, La Jolla, California 92093-0401

(Received 4 October 1999)

The nature of the interfacial exchange between a ferromagnetic (FM) metal film and an antiferromagnetic oxide film was investigated in FM (30 nm)/CoO (30 nm) bilayer films, with the FM materials Fe, Co, Ni, Ni₈₀Fe₂₀, and Ni₅₀Co₅₀. FM materials with a high Ni concentration exhibit reduced values of net unidirectional interfacial exchange energy density, $\Delta\sigma$. Mean-field analysis predicts the variation in $\Delta\sigma$ and indicates that the interfacial coupling occurs via direct exchange between metal atoms. An alternative, possibly coexisting mechanism involves plausible interfacial chemical reactions.

Exchange anisotropy¹ refers to phenomena produced by the exchange interactions at an interface between ferromagnetic (FM) and antiferromagnetic (AFM) materials. Cooling a thin-film FM/AFM bilayer in a saturating magnetic field from a temperature T intermediate between the FM Curie temperature T_C and the AFM Néel temperature T_N produces a unidirectional anisotropy that is manifested as a $\sin\theta$ torque component and a hysteresis loop displaced along the field axis. The loop shift is called the exchange field H_E . Since this loop shift is equivalent to a bias field on the FM, AFM films are widely used to bias FM sensor films in magnetoresistive read heads in current high-density information storage systems.² For this reason, investigation of exchange anisotropy phenomena has become an extremely active research topic. Assuming Heisenberg exchange across an epitaxial atomically smooth FM/AFM interface,

$$H_E = \frac{\Delta\sigma}{M_{\text{FM}}t_{\text{FM}}} = \frac{J_{\text{ex}}\mathbf{S}_i \cdot \mathbf{S}_j}{a^2 M_{\text{FM}}t_{\text{FM}}}, \quad (1)$$

where $\Delta\sigma$ is the net interfacial exchange energy density (per unit interfacial area), J_{ex} is the interfacial exchange integral, \mathbf{S}_i and \mathbf{S}_j are the spins of the interfacial atoms, a is the lattice parameter, and M_{FM} and t_{FM} are the magnetization and thickness of the FM layer, respectively. Observed exchange fields, however, are typically less than a few percent of the values predicted by this ideal interface model with a J_{ex} that is an average of the FM and AFM exchange integrals. This discrepancy is explained by the fact that the operative interfacial AFM spins are the uncompensated spins, a small fraction of all AFM surface spins, as we recently reported for polycrystalline permalloy/CoO bilayers.³ However, the nature of the interfacial FM-AFM exchange interaction was not resolved by that investigation.

The issue of interface exchange is a formidable problem. The metal-oxide interface is expected to have nonbulk properties, multiphase environments, stress gradients due to significant lattice mismatch between oxides and metals, and various types of structural defects. These features would enormously complicate rigorous modeling even if they were

well characterized. However, the techniques to provide detailed structural and chemical information at an atomic level about such a buried metal-oxide interface are not as yet well developed. This paper reports an investigation of the nature of the interfacial exchange interaction responsible for exchange anisotropy which is based on examining the behavior of H_E as the composition of the FM film was varied while keeping the AFM (CoO) film constant. A mean-field analysis demonstrates that the observed dependence of H_E on the type of FM film is inconsistent with a superexchange interaction, which might be expected at a metal-oxide interface, but correlates experimentally with a direct exchange mechanism. This analysis predicts the observed decrease in $\Delta\sigma$ with increasing Ni concentration in the FM. In addition, an alternative successful model for the dependence of $\Delta\sigma$ and $H_E(T)$ with FM composition is developed, based on very plausible chemical reactions at the metal-oxide interface. This second model also explains the dependence of $\Delta\sigma$ on the FM film at low temperatures. Both mechanisms can be operative simultaneously.

A series of films was deposited with the structure SiO₂ (20 nm)/FM (30 nm)/CoO (30 nm), where FM=Fe, Co, Ni, permalloy (Ni₈₀Fe₂₀) and Ni₅₀Co₅₀. The substrates were Si(100) wafers with a native amorphous oxide layer (~2.5 nm) which results in polycrystalline films. The films were deposited at ambient temperature with a rotating substrate table (~0.6 Hz). The CoO base layers were reactively dc sputtered.⁴ Standardized deposition conditions were used for the initial 30 nm CoO layer to insure similar magnetic and structural properties. Each FM film was dc sputtered from a single target. The substrates were backed by Alnico magnets during deposition to induce an easy axis in the FM. The SiO₂ layer was rf sputtered from an SiO₂ target and served as an effective oxidation barrier. The deposition rates were ~2.7 nm/min for the CoO and ~1.5 nm/min for the FM. CoO is an fcc type II AFM with two magnetic sublattices for $T \leq T_N = 293$ K. The AFM ordering is characterized by FM aligned (111) spin planes with adjacent antiparallel (111) planes. The AFM alignment results from the superexchange coupling of the cobalt cations via the p orbitals of the oxygen atoms.

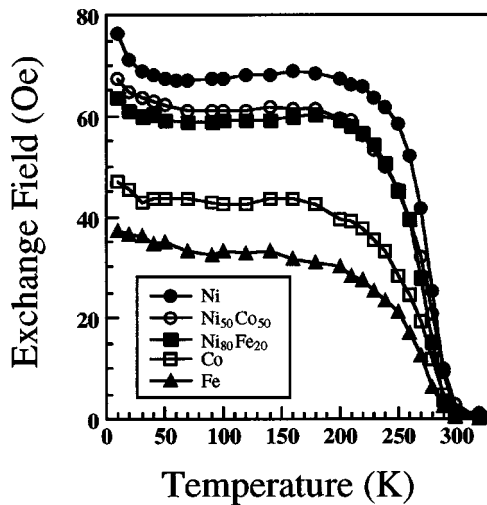


FIG. 1. Temperature dependence of H_E for FM (30 nm)/CoO (30 nm) bilayers for the FM: Ni, $\text{Ni}_{50}\text{Co}_{50}$, $\text{Ni}_{80}\text{Fe}_{20}$, Co, and Fe.

In high-angle x-ray-diffraction measurements of the bilayer films, the CoO diffraction pattern was consistent for all films as expected, and no evidence for any phases other than CoO and the FM was detected. The various FM layers are nonepitaxial to the CoO base layer and have different cubic structures: fcc (Ni, $\text{Ni}_{50}\text{Co}_{50}$, $\text{Ni}_{80}\text{Fe}_{20}$), bcc (Fe), and hcp (Co). Growth by close-packed planes was indicated by the preferred orientations of the FM materials.

Magnetic measurements were made with an alternating gradient magnetometer (AGM) and a superconducting quantum interference device (SQUID) magnetometer. Room temperature measurements using a calibrated AGM verified that the FM layers exhibited M_S values within uncertainty (a few percent) of the published literature values.⁵ The published M_S values are used in the analysis. The temperature dependencies of H_E were obtained from a series of hysteresis loops measured using a SQUID magnetometer at temperatures ranging from 10 to 320 K after field-cooling from 340 K ($>[T_N + 45 \text{ K}]$) to 10 K in a +10 kOe field. The FM easy axis was aligned parallel to the measurement field. The temperature above which H_E is zero is defined as the blocking temperature (T_b).

Figure 1 shows $H_E(T)$ for the FM/CoO bilayer films. The $H_E(T)$ curves for the FM/CoO films are qualitatively similar and share three common features: (i) $T_b = 295 \pm 5 \text{ K}$ which agrees with the bulk T_N of CoO; (ii) an intermediate temperature region ($200 \text{ K} \geq T \geq 50 \text{ K}$) in which $H_E(T)$ is independent of temperature (a “plateau” feature); and (iii) a low-temperature increase of $H_E(T < 50 \text{ K})$. The plateau and low temperature features of H_E were also observed in identical temperature regions of the magnetization of the uncompensated surface spins of CoO layers.³ The two features correspond to two different interfacial uncompensated CoO spin populations. The AFM spins responsible for the plateau feature are coupled strongly to the spins in the CoO core and are characterized by large anisotropy fields and a high magnetic ordering temperature ($\sim T_N$). The AFM spins responsible for the low-temperature increase are characterized by moderate anisotropy fields and low “freezing” temperatures; thus, we infer that these spins are weakly coupled to the core of the CoO layers.

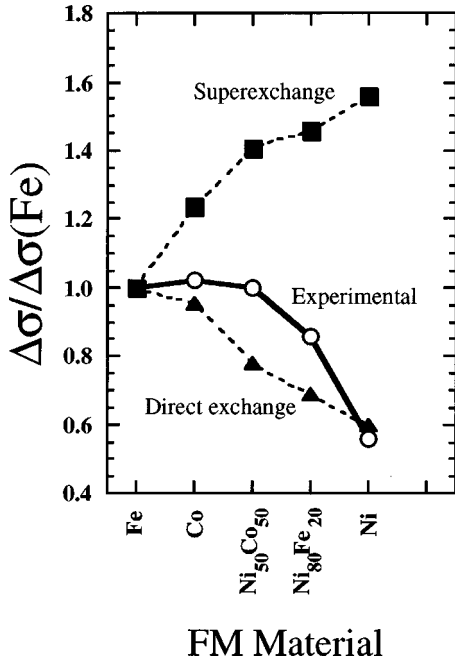
TABLE I. Magnetization data of FM (30 nm)/CoO (30 nm) bilayers.

FM	Bulk M_S (emu/cc) $T = 0 \text{ K}$	H_E (Oe) $T = 50 \text{ K}$	$\Delta\sigma$ (erg/cm ²)	$\frac{\Delta\sigma}{\Delta\sigma(\text{Fe})}$
Fe	1745	35.0	0.183	1.00
Co	1435	43.5	0.187	1.02
$\text{Ni}_{50}\text{Co}_{50}$	974	62.5	0.183	1.00
$\text{Ni}_{80}\text{Fe}_{20}$	893	59.0	0.158	0.86
Ni	512	67.3	0.103	0.56

The qualitative similarities of $H_E(T)$ for the various FM materials strongly suggest a common exchange coupling mechanism for all films. The values of H_E were analyzed to determine the possible roles of the interfacial exchange parameters. Table I lists the values of $\Delta\sigma$ from Eq. (1) using the measured $H_E(50 \text{ K})$, which is representative of the “plateau” value. $\Delta\sigma$ is shown normalized to the value for Fe in the last column of Table I. The $\Delta\sigma$ values for Fe, Co, and $\text{Ni}_{50}\text{Co}_{50}$ are within 2% of each other, whereas the values for permalloy and Ni are considerably lower (i.e., the normalized values are 86 and 56%, respectively). Thus, FM materials with the highest concentration of Ni have lower values of $\Delta\sigma$. The model of strong antiferromagnetic interfacial exchange by Mauri *et al.*⁶ predicts a constant value of $\Delta\sigma$ for all FM/CoO bilayers due to the limitation imposed by the formation of an interfacial 180° AFM domain wall during the reversal of the FM layer. The observed variation of $\Delta\sigma$ values with the various FM materials, however, suggests a dependence of $\Delta\sigma$ on the interfacial exchange parameters. The model by Mauri *et al.*⁶ predicts a linear dependence of $\Delta\sigma$ on interface coupling for the case of relatively weak interfacial exchange across a flat, uncompensated boundary. The model by Malozemoff⁷ predicts a weaker dependence on interface exchange coupling across a rough interface.

The interfacial exchange integral parameters J_{ex} were derived from a mean-field analysis. The interfacial coupling between the interfacial spins \mathbf{S}_j and \mathbf{S}_j was modeled with the assumption of a binary alloy of Co and FM atoms. A mean-field analysis was applied to two possible interfacial configurations, which would exhibit either superexchange or direct exchange coupling. In superexchange, the interfacial exchange between an AFM Co atom and an FM metal atom is mediated by an oxygen atom ($\text{Co}^{2+}\text{-O}^{2-}\text{-FM}^{2+}$). In direct exchange, the AFM Co atom couples directly to the FM metal atom (Co-FM). In the superexchange case, the interfacial spins are AFM aligned; whereas, in the direct exchange case, the interfacial spins are FM aligned. Several other basic assumptions were used: (i) each atom has a specified number of nearest neighbors (nn) and next-nearest neighbors (nnn); (ii) the minimum number of exchange interactions appropriate to the type of exchange were used to model the system (e.g., the FM environment can be described by a single interaction effective only between nn atoms); and (iii) all nn and/or nnn across the interface are those of the other interfacial component.

We first consider the case of interfacial superexchange. In CoO, the nn and nnn Co^{2+} ions are, respectively, connected by 90° and 180° $\text{FM}^{2+}\text{-O}^{2-}\text{-FM}^{2+}$ paths involving one inter-



FM Material

FIG. 2. Interfacial exchange energy densities for the various FM materials. The experimental data (solid line) are compared to the calculated values for the two interfacial coupling models—superexchange and direct exchange. For each interface model, the interfacial exchange energy density for each material was normalized to the experimental value of $\Delta\sigma$ (Fe).

mediate O^{2-} ion. CoO has two superexchange interactions: (i) J_1 is a weak AFM interaction between nn, and (ii) J_2 is a strong AFM interaction between nnn. We assume the interfacial magnetic structure is also fcc type II and employ the bulk analysis for the interfacial atoms. The Néel temperature (\bar{T}_N) for a hypothetical material of the interfacial alloy composition would be given by⁸

$$\bar{T}_N \propto \frac{\bar{S}(\bar{S}+1)}{k_B} J_2, \quad (2)$$

where \bar{S} is the spin of the interfacial oxide composition. The nearest-neighbor terms cancel due to the spin structure in the magnetically ordered state. Solving for $J_2 = J_{ex}$ and substituting into Eq. (1), the interfacial exchange energy density $\Delta\sigma$ has the form

$$\Delta\sigma \propto \frac{\bar{S}}{\bar{S}+1} \bar{T}_N. \quad (3)$$

The values of \bar{T}_N for the AFM oxide alloys vary linearly with composition,⁹ so \bar{T}_N is equal to the average T_N of CoO and FM-O. \bar{S} was calculated by using the stoichiometric average of the Co^{2+} and FM^{2+} spin values, as determined by neutron diffraction.¹⁰ For the cases of interfacial superexchange, the upper curve in Fig. 2 shows the calculated ratios of $\Delta\sigma$ normalized to the experimental value of $\Delta\sigma$ (Fe). The high T_N for NiO relative to CoO results in higher \bar{T}_N values for FM materials with higher Ni concentrations. The interfacial AFM coupling configuration predicts an increasing rela-

tive trend for $\Delta\sigma$ for FM materials with higher Ni concentration; this contrasts strongly with the measured results.

For the case of direct exchange, mean-field theory utilizes a single FM exchange J between nn atoms. One finds⁸

$$\bar{T}_C \propto \frac{\bar{S}(\bar{S}+1)}{k_B} J, \quad (4)$$

which is the same formulation as for the AFM, where \bar{T}_C and \bar{S} are the average Curie temperature and the average spin of the interfacial metal composition, respectively. The analogous expression for $\Delta\sigma$ is

$$\Delta\sigma \propto \frac{\bar{S}}{\bar{S}+1} \bar{T}_C. \quad (5)$$

The spin \bar{S} satisfies $\mu = g\mu_B\bar{S}$ for the bulk interfacial metallic composition. The Curie temperatures and atomic magnetic moments of the various FM alloys were obtained from the literature.⁵ In Fig. 2, the calculated ratios of $\Delta\sigma$ with respect to $\Delta\sigma$ (Fe) for direct exchange predict the correct trend of decreasing $\Delta\sigma$ for FM with increasing Ni concentration. The lower $\Delta\sigma$ values of the FM materials with higher Ni concentrations reflect their lower Curie temperatures and spin values.

The inferred direct metal-metal interfacial bond is somewhat unexpected for an oxide-metal interface. A local balance in the number of oxygen and metal ions on the oxide surface is required to minimize surface energy due to charging, so the condition of an oxide free interface between the FM and the AFM Co atoms is improbable. RHEED analyses of the surface (111) spin plane of NiO (Ref. 11) and MgO (Ref. 12) indicate a rapid interfacial restructuring, observed as superstructure in the RHEED pattern, to reduce this electrical charge.¹⁰ Thus, an oxygen-free direct exchange would suggest that a fraction of the initial atomic layer of FM atoms becomes incorporated as the upper surface of the AFM layer.

The result of FM direct exchange coupling at the CoO-FM interface is in contrast to the interfacial AFM interactions suggested by Nogués *et al.*¹³ in the single-crystal FeF_2 -Fe system. Nogués *et al.* reported a negative to positive exchange bias transition with increasing cooling field and suggested an AFM FeF_2 -Fe interfacial coupling as an explanation. We found, however, that the permalloy/CoO bilayer films exhibited negative exchange biasing and no dependence of H_E on the magnitude of the applied cooling field ($50 \text{ kOe} > H_{cool} > 50 \text{ Oe}$).¹⁴ Since a cooling field of 50 Oe is sufficient to magnetically saturate the permalloy layer, the permalloy is in a single domain state during the field-cooling process.

While direct exchange accounts for the observed variation in $\Delta\sigma$, an alternative explanation can be given in terms of chemical reactions at the FM-AFM interface. The elevated surface temperature caused by the kinetic energy and heat of condensation of the sputtered FM films can lead to FM oxidation. Partial oxidation of the FM at the interface has been seen¹⁵ in ^{57}Fe Mössbauer measurements on Ni (15 nm)/ $^{57}Fe(t)$ /CoO (30 nm) for ^{57}Fe thicknesses $0.4 \leq t \leq 1.6$ nm. These reactions can modify the surface of the CoO films to provide for better FM-AFM coupling. For FM=Co

and Fe, the marked increase in $\Delta\sigma$ and strong decrease in the low-temperature rise in H_E are consistent with this model. A variation on this model would note the possibility of a thin layer of Co_3O_4 on the surface of the newly formed CoO, due to the ready oxidation¹⁶ of the CoO surface in the reactive sputtering gas. Bulk Co_3O_4 has $T_N=30$ K,¹⁷ slightly below the observed onset of H_E increase. The thin Co_3O_4 layer is expected to have a somewhat larger blocking temperature than bulk Co_3O_4 due to its strong exchange coupling with the higher T_N CoO, similar to the increase in apparent T_N for $\text{Fe}_3\text{O}_4/\text{CoO}$ superlattices.¹⁸ During subsequent FM film deposition, the FM and Co_3O_4 could react to form monoxides. The new monoxide layer would provide a more direct FM-AFM exchange coupling, increasing measured H_E and decreasing the low-temperature rise in H_E . Furthermore, the strongest fractional temperature dependence for $T>100$ K is seen for FM=Fe, which is expected since FeO exhibits the lowest T_N (≈ 200 K) of the pure $3d$ monoxides. The reason why the film with FM=Ni does not seem to show the interface reactivity may be due to the difficulty in forming intermediate Ni-Co spinels,¹⁹ or the relatively low diffusion coefficients in mixed monoxides.²⁰ Note that the interface reaction layer might exhibit topographic morphologies different than the underlying CoO film, depending on the particular reactants. This could change the surface density of

uncompensated spins, and, hence, modify H_E .

In summary, we measured a dependence of the interfacial energy density $\Delta\sigma$ on the FM material in FM/CoO bilayer films. The bilayer films with FM materials containing higher concentrations of Ni exhibit lower values of $\Delta\sigma$. Two models were discussed which predict the observed behavior. In one, mean-field calculations account for the variation with a model of a limiting interfacial environment composed of an alloy of Co and FM metal atoms coupled by direct exchange. This result is contrary to expectations for a metal/oxide interface. Despite the large degree of spin compensation of the AFM interface, the result of interfacial direct exchange implies that the net or uncompensated AFM spins responsible for the unidirectional anisotropy are parallel to the FM spins. In the alternative model, chemical reaction of the FM metal atoms with the top layer of Co_3O_4 , which seems to be present on the CoO, can be very plausibly associated with the observed dependence of $\Delta\sigma$ with the FM. Both of these mechanisms may be present simultaneously, and both emphasize the importance of the interfacial species in determining the magnitude of the exchange field.

This work was supported in part by the NSF-MRSEC Program DMR-9400439 and the ATP Heads Program administered by NSIC.

*Present address: IBM-Almaden Research Center, 650 Harry Road K63/E3, San Jose, CA 95120.

¹W. H. Meiklejohn and C. P. Bean, Phys. Rev. **102**, 1413 (1956); **105**, 904 (1957).

²B. Dieny, V. S. Speriosu, S. S. P. Parkin, B. A. Gurney, D. R. Wilhoit, and D. Mauri, Phys. Rev. B **43**, 1297 (1991).

³Kentaro Takano, R. H. Kodama, A. E. Berkowitz, W. Cao, and G. Thomas, Phys. Rev. Lett. **79**, 1130 (1997); J. Appl. Phys. **83**, 6888 (1998).

⁴M. J. Carey and A. E. Berkowitz, Appl. Phys. Lett. **60**, 3060 (1992).

⁵R. M. Bozorth, *Ferromagnetism* (Van Nostrand, Princeton, 1951).

⁶D. Mauri, H. C. Siegmann, P. S. Bagus, and E. Kay, J. Appl. Phys. **62**, 3047 (1987).

⁷A. P. Malozemoff, Phys. Rev. B **35**, 3679 (1987).

⁸J. S. Smart, *Effective Field Theories of Magnetism* (W. B. Saunders Co., London, 1966).

⁹*Magnetic Properties of Non-Metallic Inorganic Compounds Based on Transition Elements*, edited by G. Albanese *et al.*, Landolt-Bornstein, New Series, Group III, Vol. 27, Pt. g (Springer-Verlag, Berlin, 1992).

¹⁰W. L. Roth, Phys. Rev. **110**, 1333 (1958).

¹¹N. Floquet and L.-C. Dufour, Surf. Sci. **126**, 543 (1983).

¹²M. Gajdardziska, P. A. Crozier, and J. M. Cowley, Surf. Sci. **248**, L259 (1991).

¹³J. Nogués, D. Lederman, T. J. Moran, and I. K. Schuller, Phys. Rev. Lett. **76**, 4624 (1996).

¹⁴Kentaro Takano (unpublished).

¹⁵K. Takano, F. T. Parker, and A. E. Berkowitz, J. Appl. Phys. **81**, 5262 (1997).

¹⁶G. A. Carson, M. H. Nassir, and M. A. Langell, in *Evolution of Thin-Film and Surface Structure and Morphology*, edited by B. G. Demczyk *et al.*, MRS Symposia Proceedings No. 355 (Materials Research Society, Pittsburgh, 1994).

¹⁷L. M. Khriplovich, E. V. Kholopov, and I. E. Paukov, J. Chem. Thermodyn. **14**, 207 (1982).

¹⁸Y. Ijiri, J. A. Borchers, R. W. Erwin, S. H. Lee, P. J. van der Zaag, and R. M. Wolf, J. Appl. Phys. **83**, 6882 (1998).

¹⁹P. Peshev, A. Toshev, and G. Gyurov, Mater. Res. Bull. **24**, 33 (1989).

²⁰H. Matzke, in *Nonstoichiometric Oxides*, edited by O. T. Sorensen (Academic Press, New York, 1981), p. 155.